Journal of Engineering Research and Reports

Volume 26, Issue 9, Page 88-104, 2024; Article no.JERR.121200
ISSN: 2582-2926

Design and Simulation of an Innovative Modular Four-Bar Linkage Robotic Arm: Analysis and Applications

Jiajun Ma [a*], Ziqi Luo [a], Chuan Ding [a] and Huimin Yuan [a]

[a] School of Mechanical Engineering, North China University of Water Resources and Electric Power, Zhengzhou -450045, China.

Authors' contributions

This work was carried out in collaboration among all authors. All authors read and approved the final manuscript.

Article Information

DOI: https://doi.org/10.9734/jerr/2024/v26i91266

Open Peer Review History:
This journal follows the Advanced Open Peer Review policy. Identity of the Reviewers, Editor(s) and additional Reviewers, peer review comments, different versions of the manuscript, comments of the editors, etc are available here: https://www.sdiarticle5.com/review-history/121200

Original Research Article

Received: 24/06/2024
Accepted: 28/08/2024
Published: 01/09/2024

ABSTRACT

In response to the issues of traditional manipulators, such as difficulty in controlling the terminal posture during motion, low control precision, and complex structure, a modular mechanical arm based on a parallel four-bar terminal posture maintenance mechanism has been designed to meet the special requirements of terminal posture maintenance. By analyzing the motion mechanism of the manipulator, the shape space of the manipulator, the terminal position space, and the relationships of forward and inverse kinematics have been derived. A simulation model of the linkage manipulator was established in the Robotic Toolbook for Matlab environment, and structural simulation analysis and kinematic equation verification were conducted. The end positioning and attitude control of different manipulators are simulated by Matlab programming. The working space of the manipulators is calculated by Monte Carlo method, and compared with that of traditional planar manipulators. The results show the validity of the kinematics equation and the rationality of

**Corresponding author: Email: 1491155742@qq.com;*

Cite as: *Ma, Jiajun, Ziqi Luo, Chuan Ding, and Huimin Yuan. 2024. "Design and Simulation of an Innovative Modular Four-Bar Linkage Robotic Arm: Analysis and Applications". Journal of Engineering Research and Reports 26 (9):88-104. https://doi.org/10.9734/jerr/2024/v26i91266.*

the end positioning control scheme of the linkage manipulator. Finally, the experiment verifies that the attitude retention rate of the modular decoupling manipulator is 97.78% under high load, which verifies the reliability of this scheme. In addition, the manipulator can simplify the complexity of the mechanical structure and complete the control requirements of the terminal attitude under the premise of increasing the working space as much as possible, which lays a foundation for the design and optimization of the manipulator in the field of modular terminal attitude.

Keywords: Attitude control; modular robotic; kinematics analysis; structural simulation.

1. INTRODUCTION

As technology races forward, robotic arm technology has emerged as an integral part of the automation and robotics sectors, playing a vital role in pivotal industries such as medicine, emergency response, and outer space exploration [1,2]. In the realm of industrial manufacturing, robotic arms are also instrumental in tasks like assembly, transportation, and welding, significantly boosting production efficiency and ensuring safety standards [3].

With the increasing application of robotic arms, the requirements for robotic arms are also increasing, in many research and practical application scenarios; For example, in scenarios such as picking operations in precision agriculture, engineering hair chisel operations and medical surgery operations, the robotic arm needs to control the attitude of its end working platform to maintain or transform it to a specific Angle to meet the needs of the above special work scenarios [4].

The control methods for the end posture of the manipulator are as follows:

Decoupling Through Special Mechanical Arm Structural Design: Feng Xu designed and implemented a 7-DOF cable-driven painting robot with a motion-decoupling mechanism. The innovative mechanical structure effectively solved the coupling issues in the motion of cable-driven joints, enhancing the robot's flexibility and precision, but the complexity of the arm structure at various levels remains an issue [5].

Xin-Jun Liu proposed a 2-DOF planar parallel manipulator with three parallelograms, using parallelograms to decouple the serial mechanical arm and give it the properties of a parallel mechanical arm, thus stabilizing the end posture. However, it has a dead zone at the top and limited joint rotation angles [20°-160°] [6].

Decoupling Through Joint Motor Control: Guangyu Zhang introduced a new design for a 9-DOF upper limb rehabilitation robotic arm, which completes the requirements of human body rehabilitation by controlling the joint motors to perform linear and rotational movements of the mechanical arm [7]. Runtong Sun presented a dynamic control design method for a hybrid painting robot containing parallelogram linkages, leveraging its unique dynamic characteristics such as time invariance, joint independence, and linear approximability to achieve high-performance control, improving the tracking accuracy and motion consistency of the robot [8]. However, this approach has high demands on the upper computer and weaker robustness in kinematic analysis.

Nevertheless, these methods have certain limitations. They typically rely on the mutual coupling control of motors, which not only makes posture control more complex but also often results in unsatisfactory positioning accuracy. At the same time, although the use of posture retention mechanisms can improve posture accuracy, these mechanisms often lead to more complex individual designs for each level of the mechanical arm, and issues such as mutual collision of links and entanglement of cables, which limit the working range and increase control difficulty.

In summary, to address these issues, it is necessary to manufacture a modularly decoupled mechanical arm. Combining modularization with end-posture maintenance mechanisms is an effective solution. By modularizing the various levels of the mechanical arm, not only can the complexity of the mechanism be simplified, but also the working range of the mechanical arm can be expanded. At the same time, compared with decoupling through control algorithms, a modularly decoupled mechanical arm can reduce the number of motors, thereby lowering costs. Additionally, because each level of the mechanical arm is independent, the complexity

of control programming can be effectively reduced.

From an application perspective, in certain specific application scenarios that require the mechanical arm to maintain a certain stable end posture, such as concrete chiseling and kiwi picking, a modularly decoupled mechanical arm has the aforementioned advantages. It can not only maintain the end posture through mechanical mechanisms but also, because each level of the mechanical arm can maintain a relatively independent posture, it has significant advantages in reducing the complexity of designing mechanical arm control systems, as well as subsequent research and development.

To further the study of the modularly decoupled mechanical arm, a detailed investigation will be conducted by analyzing the working mechanism, forward and inverse kinematics, and the workspace of the proposed mechanical arm. The workspace of the mechanical arm is a critical kinematic indicator that measures its operational capability, covering the spatial area that the end-effector can reach under all possible movements [9-11].

Methods for determining the workspace mainly include geometric construction, analytical methods, and numerical computation. The geometric construction method is intuitive and easy to understand but computationally complex and difficult to apply for accurately representing complex shapes. Analytical methods can provide precise boundaries, but their computational complexity increases with the number of joints.

The Monte Carlo method involves random sampling across the range of values for each joint of the mechanical arm, and the collection of endpoint values constitutes the workspace of the mechanical arm. This random sampling method can approximate the workspace with a relatively small computational load and at a faster speed. Moreover, the reliability of the representation of the workspace surface can be improved by increasing the number of samples [12-14]. Therefore, this paper employs the Monte Carlo method for solving the workspace.

In terms of simulation verification, this paper utilizes the Robotic Toolbook for Matlab platform to establish a simulation model of the mechanical arm based on the derived inverse kinematics model and conducts simulation analysis for end-point positioning. According to the experimental results, the posture retention rate remained above 97.78% in all tests, indicating that the robotic arm can maintain good posture control performance at each stage. This proves the effectiveness of the modular mechanical decoupling scheme. By deriving its shape space, end position space, and the relationships of forward and inverse kinematics, this study lays a theoretical foundation for the subsequent design and optimization of modular mechanical structure decoupled mechanical arms.

2. STRUCTURAL DESIGN

In response to tasks that necessitate a stable end posture, we have engineered a modular parallel robotic arm architecture. To simplify component and structural complexity while also improving the arm's payload capacity within the power constraints of the motors, aluminum alloy has been selected as the construction material. The robotic arm is unified through servos, couplings, and an axis at the base of the swing arm to transmit torque. It is connected to the misaligned connection mechanism above via bearings integrated into the arm, and three misaligned connection mechanisms serve as the short sides of the parallel four-bar linkage, linked to the long lead screw, to maintain the arm's terminal posture through the parallelogram principle. For instance, with the primary and secondary robotic arms, the rotation of the primary arm, aided by the posture retention mechanism, ensures the upper platform remains parallel to the swing arm base plate at all times; the rotation angle of the primary arm influences only the position, not the posture, of the secondary arm.

Throughout this study, the structure of each robotic arm level is fundamentally identical, each equipped with a dedicated servo motor mounting plate. The primary and secondary arms are powered by the TD-8135MG servo motor from TIANKONGRC, whereas the tertiary arm utilizes the TD-8115MG servo motor. A 16-channel PWM Servo motor driver board is employed as the driving unit.

In the realm of modular robotic arms, achieving precise end-effector positioning is a prevalent concern. Conventionally, these arms rely on an array of motors and sophisticated control algorithms to fine-tune the joint motor angles, ensuring a stable end posture. However, this method can be prohibitively expensive.

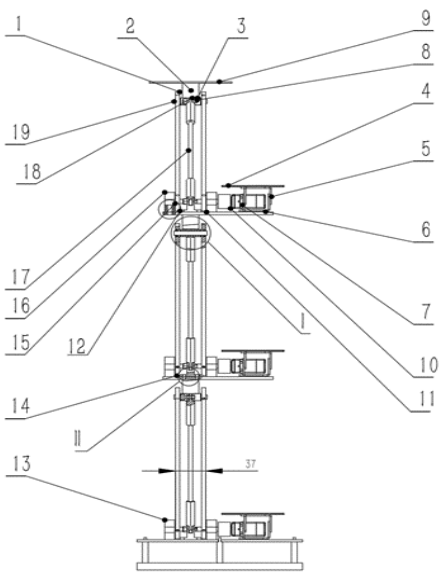

Fig. 1. Structural design of robotic arm

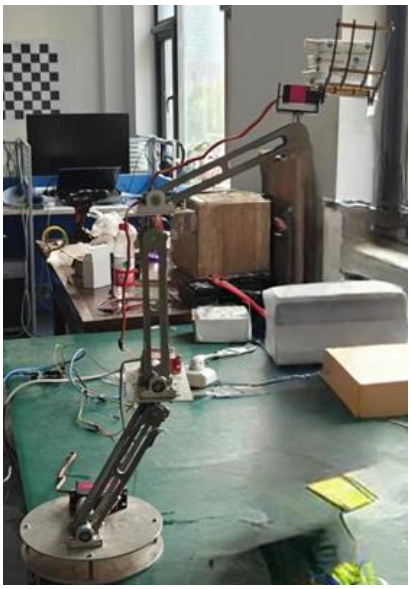

Fig. 2. Design model of robotic arm

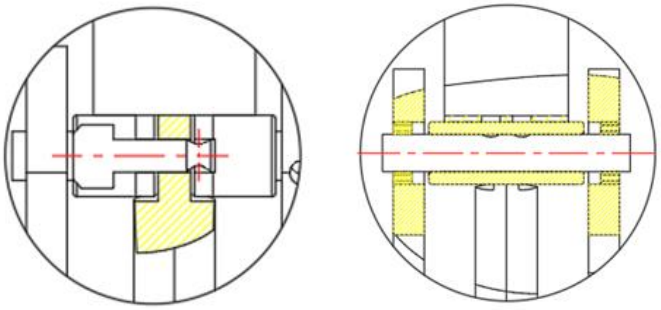

To address this, the integration of modular robotic arms with end posture retention mechanisms is proposed. This not only broadens the operational workspace but also guarantees the accuracy of end-effector positioning. The mechanism employed in this study is a parallelogram structure. Capitalizing on the inherent geometric properties of parallelograms, this structure, composed of two or more parallelograms, facilitates both translational and rotational movements of the robotic arm. By employing this structure to maintain the arm's posture, the complexity of the control algorithms for posture management is significantly reduced.

3. KINEMATIC ANALYSIS

3.1 Geometric Relationship Analysis and Kinematic Modeling

During the execution of tasks, the workspace of a robotic arm plays a crucial role in its performance analysis. To solve for the workspace of the robotic arm, one must solve the kinematic equations of the arm. This process begins with an analysis of the robot, calculating the homogeneous transformation matrix from known joint angles to determine the pose of the end-effector. Due to the complexity and intricacy of the geometric parameters of a robotic arm, coordinate systems are typically constructed for each link, with the geometric parameters of the arm expressed through the relationships between these coordinate systems. The widely used model is the D-H (Denavit-Hartenberg) model proposed by Daneivt and Hartenberg [15]. As shown in Fig. 3, the parameters of the modular robotic arm model are listed in Table 1. Based on the DH parameters, we use MATLAB’s Robotics Toolbox for robot simulation to simulate the kinematics and trajectory planning of the robotic arm. Utilizing functions such as LINK() [16,17], ROBOT(), DISPLAY(), and TEACH()

from the MATLAB simulation toolbox, we program a kinematic simulation model of the robotic arm, controlling the control panel for each joint angle and the coordinate parameters of the end-effector's pose. As shown in Table 1.

3.2 Forward Kinematic Analysis

In robotic kinematics, the spatial transformation of a point is an amalgamation of translational and rotational components. The posture of a rigid body is encapsulated by a matrix that encompasses both a position vector and three directional vectors. To articulate the posture of a robotic manipulator, we employ homogeneous transformation matrices, which denote the coordinate transformation from the rigid body coordinate system {A} in relation to the reference coordinate system {O}.

Table 1. D-H parameters of the robotic arm

l_i	α_i / (°)	α_i /mm	d_i /mm	θ_i /(°)	Joint range/(°)
1	0	0	10	θ_1	[-150,150]
2	0	200	0	θ_2	[-150,150]
3	0	200	0	θ_3	[-150,150]
4	0	200	0	θ_4	[-150,150]

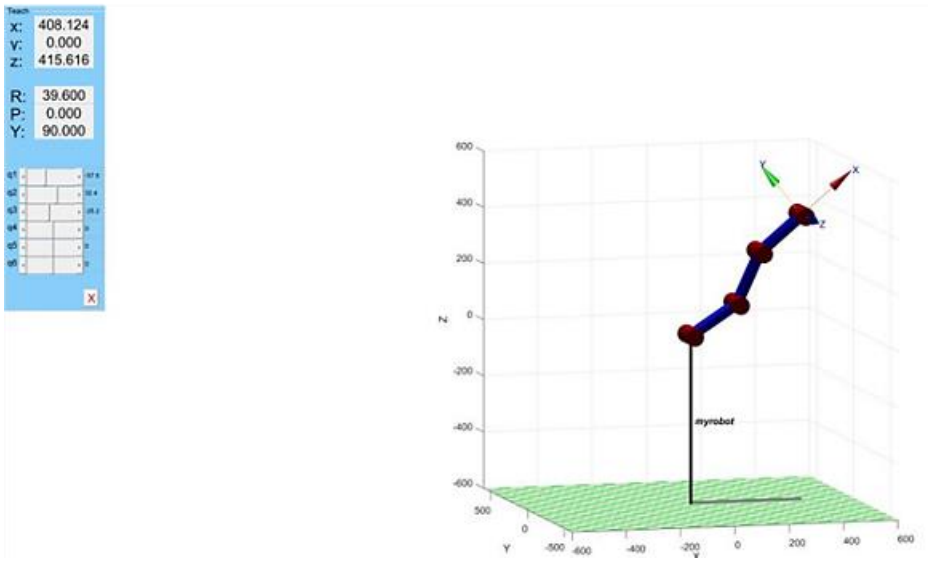

Fig. 3. D-h modeling of modular robotic arm

$$ {}^{O}_{A}T = \begin{bmatrix} r_{11} & r_{12} & r_{13} & P_X \\ r_{21} & r_{22} & r_{23} & P_Y \\ r_{31} & r_{32} & r_{33} & P_Z \\ 0 & 0 & 0 & 1 \end{bmatrix}, \tag{1} $$

To simplify the expression and enhance clarity in the subsequent calculations, we will use s_i and c_i to denote $\sin(\theta_i)$ and $\cos(\theta_i)$, respectively. Additionally, we will use s_{mn} and c_{mn} to represent $\sin(\theta_m + \theta_n)$ and $\cos(\theta_m + \theta_n)$, respectively. By substituting into the aforementioned formula, we can ascertain the homogeneous transformation matrices for each of the robot's joints.

$$ {}^{0}_{1}T = \begin{bmatrix} c\theta_1 & -s\theta_1 & 0 & 0 \\ s\theta_1 & c\theta_1 & 0 & 0 \\ 0 & 0 & 1 & 0 \\ 0 & 0 & 0 & 1 \end{bmatrix}, \tag{2} $$

$$ {}^{1}_{2}T = \begin{bmatrix} c\theta_2 & -s\theta_2 & 0 & l_2 \\ s\theta_2 & c\theta_2 & 0 & 0 \\ 0 & 0 & 1 & 0 \\ 0 & 0 & 0 & 1 \end{bmatrix}, \tag{3} $$

$$ {}^{2}_{3}T = \begin{bmatrix} c\theta_3 & -s\theta_3 & 0 & l_3 \\ s\theta_3 & c\theta_3 & 0 & 0 \\ 0 & 0 & 1 & 0 \\ 0 & 0 & 0 & 1 \end{bmatrix}, \tag{4} $$

Within the context of robotic arms, the interrelation of two contiguous joint coordinate systems is articulated through homogeneous transformation matrices. Utilizing this approach, we can ascertain the transformation matrix that aligns the robot's end-effector coordinate system with the base coordinate system. In an effort to streamline the computational process, we initially engage in a matrix simplification technique:

$$ s_{12} = c_1 s_2 + s_1 c_2, \tag{5} $$

$$ c_{12} = c_1 c_2 - s_1 s_2, \tag{6} $$

$$ {}^{0}_{4}T = \begin{bmatrix} r_{11} & r_{12} & r_{13} & P_X \\ r_{21} & r_{22} & r_{23} & P_Y \\ r_{31} & r_{32} & r_{33} & P_Z \\ 0 & 0 & 0 & 1 \end{bmatrix}, \tag{7} $$

$$ \begin{cases} r_{11} = c_1 c_2 - s_1 s_2 \\ r_{21} = s_{12} c_3 + c_{12} s_3 \\ r_{31} = 0 \\ r_{12} = -c_{12} s_3 - s_{12} c_3 \\ r_{22} = -s_{12} s_3 + c_{12} c_3 \\ r_{32} = 0 \\ r_{13} = 0 \\ r_{23} = 0 \\ r_{33} = 1 \\ P_X = c_1 l_1 + c_{12} l_2 \\ P_Y = s l_1 + s_{12} l_2 \\ P_Z = 0 \end{cases}, \tag{8} $$

3.3 Inverse Kinematic Analysis

The inverse kinematics of the manipulator is analyzed by geometric method, through the analysis of Fig. 2, we can get the motion Fig. 4.

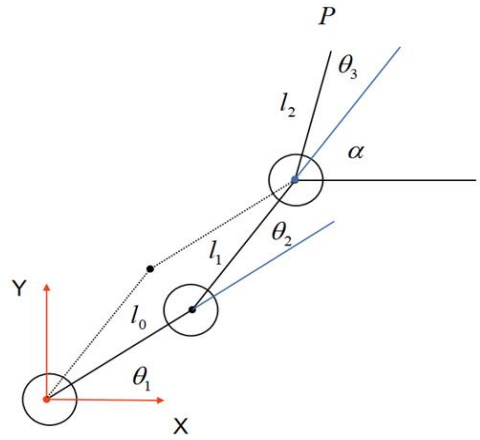

Fig. 4. Mechanical arm movement diagram

According to Fig. 4, we can list the following equation:

$$x = l_0 \cos\theta_1 + l_1 \cos(\theta_1 + \theta_2) + l_2 \cos(\theta_1 + \theta_2 + \theta_3), \tag{9}$$

$$y = l_0 \sin\theta_1 + l_1 \sin(\theta_1 + \theta_2) + l_2 \sin(\theta_1 + \theta_2 + \theta_3), \tag{10}$$

$$a = \theta_1 + \theta_2 + \theta_3, \tag{11}$$

The above equations are simplified as follows:

$$x = l_0 c_1 + l_1 \cos_{12} + l_2 c_\alpha, \tag{12}$$

$$y = l_0 s_1 + l_1 s_{12} + l_2 s_\alpha, \tag{13}$$

For ease of computation, we define:

$$m = l_2 c_\alpha - x, \tag{14}$$

$$n = l_2 s_\alpha - y, \tag{15}$$

Simplified formula:

$$l_1 = (l_0 c_1 + m) + (l_0 s_1 + n)^2, \tag{16}$$

$$k = (l_0^2 - l_1^2 - m^2 - n^2) / 2l_1, \tag{17}$$

$$s_1 = (-b \pm \sqrt{b^2 - 4ac}) / 2a, \tag{18}$$

$$m^2 + n^2 = a, \tag{19}$$

$$b = -2nk, \tag{20}$$

$$C = k^2 - m^2, \tag{21}$$

$$\theta_1 = \arcsin((-b \pm \sqrt{b^2 - 4ac}) / 2a), \tag{22}$$

$$x^2 + y^2 = l_1^2 + l_2^2 + 2 * l_1 * l_2 * c_3, \tag{23}$$

$$c_2 = (x^2 + y^2 - l_1^2 - l_2^2 2 * l_1 * l_2) / (2 * l_1 * l_2), \tag{24}$$

Considering the range $-75 < j_3 < 75^{\circ}$, we can deduce that the sine of j_3, denoted as s_3, is greater than zero.

$$s_2 = \sqrt{1 - c^2 2}, \tag{25}$$

$$\tan 2 = \frac{s_2}{c_2}, \tag{26}$$

$$\theta_2 = \arctan 2(s_2, c_2), \tag{27}$$

We presuppose that the transformation from the wrist coordinate system to the base coordinate system has been accomplished, thereby ascertaining the position of the target point. As our focus lies with a planar robotic arm, the position is readily determined by specifying the three parameters: x, y, and α.

$$a = \arctan 2(s_\alpha, c_\alpha), \tag{28}$$

$$\theta_3 = \arctan 2(s_\alpha, c_\alpha) - \theta_1 - \theta_2, \tag{29}$$

4. ROBOTIC ARM MOTION SIMULATION

4.1 Construction of Robotic Arm Simulation Model

In this paper, we utilize the simulation toolbox available on the Robotic Toolbook for Matlab platform to analyze the kinematics and workspace of the robotic arm. By employing the MATLAB simulation toolbox, we create models for all the links, which include kinematic information of the robotic arm corresponding to the DH (Denavit-Hartenberg) table. We control the coordinate parameters of the end-effector's pose through a control panel that adjusts the angles of each joint using forward kinematics [18]. As shown in Fig. 6, the control panel sets the joint angles to $\theta = (30°, 20°, 30°)$, and the end position coordinates of the robotic arm are (-268.404, 0, 534.349). To verify this result, we substitute these angles into the forward kinematic equations of the robotic arm, and the values obtained match perfectly, thereby validating the correctness of the kinematic equations for the six-axis robotic arm.

This approach not only demonstrates the practical application of the Robotic Toolbook for Matlab but also highlights the effectiveness of the MATLAB simulation toolbox in conducting kinematic analysis and confirming the accuracy of the robotic arm's motion equations.

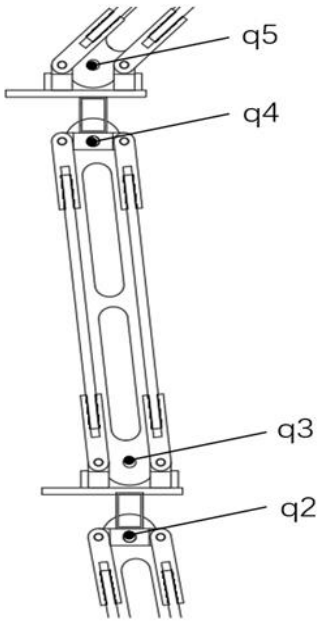

Fig. 5. Construction of robotic arm simulation model

Using the same methodology, we can construct a three-axis planar robotic arm with parallel joints, with joint twist angles denoted as q1 for the first, q2 for the second, and q4 for the third joint. For a four-axis planar robotic arm, the joints remain parallel, with joint twist angles being q1, q2, q4, and q6. Additionally, there is a structurally identical six-axis robotic arm that does not incorporate an end posture retention mechanism, with joint twist angles q1, q2, q3, q4, q5, and q6. In this six-axis robotic arm, joints q2 and q3 are positioned directly above joints q4 and q5, with a fixed distance between them. This configuration does not affect the forward kinematic calculations, and the joints are parallel to each other. To facilitate a more intuitive comparison in simulation modeling, we consider q2 and q3 as a single joint, and q4 and q5 as another joint.

This study presents a comparative analysis of the simulation models for modular three-axis parallel robotic arms (a), three-axis planar robotic arms (b), and four-axis planar robotic arms (c). The endpoint coordinates for the modular three-axis parallel robotic arm are (-268.404, 0, 534.349), with corresponding joint angles of $\theta = (30°,20°,30°)$. Conversely, the three-axis planar robotic arm necessitates accounting for the interplay among its segments, Compared with the proposed machine, decoupling operation is needed to offset the rotation Angle, so that the robot arm can reach the target position while maintaining the pose. A comparison between (a) and (b) clearly illustrates that the terminal posture of the three-axis planar robotic arm is influenced by the rotation of the preceding joint, hindering adjustments to the terminal posture upon reaching the same location.

The introduction of an end posture adjustment motor results in a four-axis planar robotic arm, capable of aligning the robotic arm's endpoint to the coordinates (-268.404, 0, 534.349), as depicted in (c). Compare it with (a) and (b), it becomes apparent that the four-axis planar robotic arm can maintain its terminal posture while arriving at the designated position. Nonetheless, in contrast to the modular three-axis parallel and three-axis planar robotic arms, the four-axis variant entails an increased number of motors. When juxtaposing the simulation model of a six-axis robotic arm (d), which lacks an end posture retention mechanism, with that of a three-axis parallel robotic arm, it is evident that the six-axis arm mirrors the scenario of the four-axis planar arm. It mitigates the impact of the upper arm on posture by augmenting the motor count. However, this scheme increases the cost and requires a separate structural design for each segment of the robot arm, complicating the overall structure of the robot arm. Consequently, in operational contexts demanding precise terminal posture control, the modular three-axis parallel robotic arm offers considerable advantages. See Table 2 for a comprehensive comparison of various robotic arms.

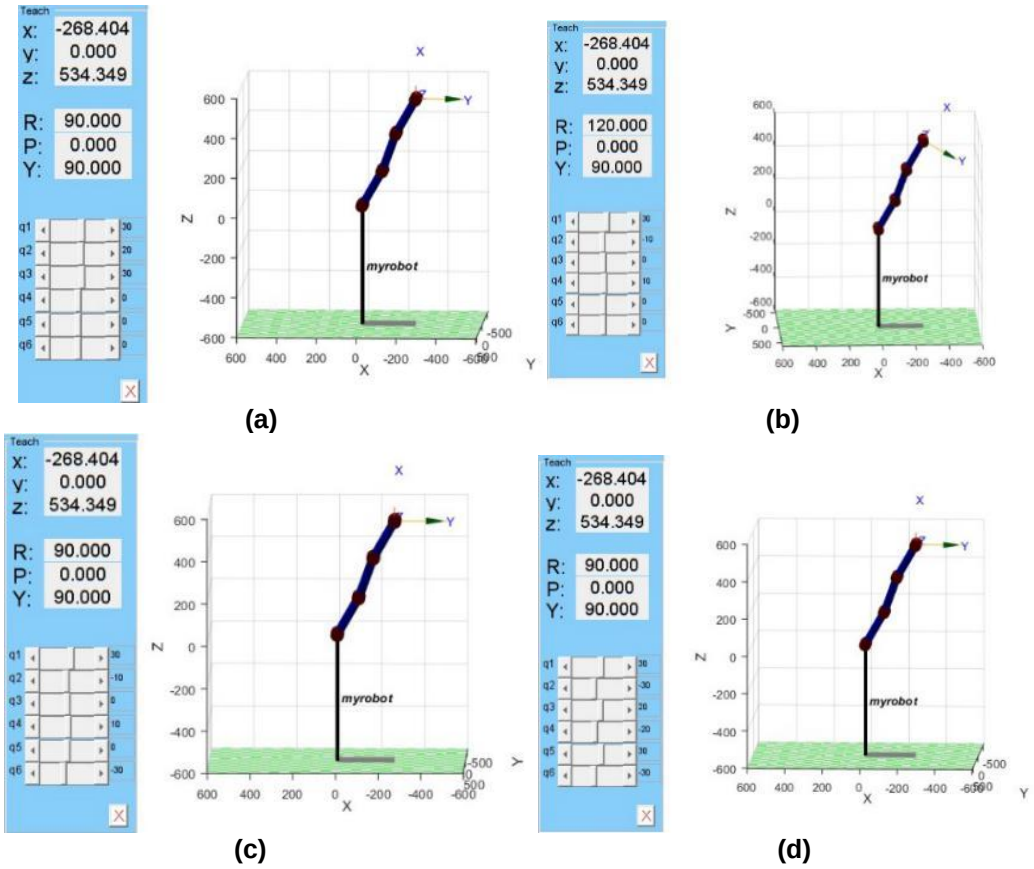

Fig. 6. Robot arm model set

Table 2. Comprehensive comparison

Manipulator structure	Number of motors	Degree of freedom	Hold posture （Y/N）	Structural complexity （1-4）	Rank the parameters of the control algorithm (1-4)	Comprehensive ranking
3-dOF plane	3	3	N	N	N	N
Modular mechanism decoupling	3	3	Y	1	1	1
4-dOF plane	4	4	Y	2	2	2
6-dOF plane	6	6	Y	3	3	3

4.2 Construction of Robotic Arm Simulation Model

The workspace of a robot is the set of all spatial points that the robot's end-effector can reach within the base coordinate system. Due to the design limitations of the robot arm, the range of motion of the robot arm is usually limited by various factors such as the structure and the motor. In this paper, the motion range of the three-axis mechanical arm is approximated by a sector, with the radius based on the length of the arm when fully extended. Due to the use of a parallelogram structure, the mechanical arm has certain joint limitations and singularities, which result in inaccessible work areas and thus restrict the workspace and flexibility of the mechanical arm. Therefore, a thorough analysis of the mechanical arm's workspace is essential. This paper focuses on the motion space issues of the modular mechanical arm within this structural context, deferring optimization problems to future research.

Common methods for analyzing the mechanical arm's workspace include analytical methods, numerical methods, and graphical methods, etc [19,20]. In this paper, we have adopted the Monte Carlo method from the category of stochastic numerical methods and implemented the construction of a point cloud model of the workspace for a six-axis mechanical arm through MATLAB programming. The following are the steps for calculating the workspace of a six-axis mechanical arm using the Monte Carlo method in MATLAB:

1) The forward kinematics of the modular three-axis robot arm is solved to obtain the end position direction the amount $\left[p_x, p_y, p_z \right]$;

2) Calculate the random value of each joint by Monte Carlo method and substitute it into the terminal position vector:

$$q_1 rand = lq_1 s + (lq_1 end - lq_1 s) * rand(num, 1)$$

$$q_2 rand = lq_2 s - q_1 rand + (lq_2 end - lq_2 s) * rand(num, 1)$$

$$q_3 rand = lq_3 s - q_2 rand + (lq_3 end - lq_3 s) * rand(num, 1)$$

In simulating the workspace of a robotic arm, we typically employ stochastic numerical methods. Here, $q_i rand$ represents the random values of joint angles, $lq_i s$ denotes the minimum values of the joint angles, and $lq_1 end$ signifies the maximum values of the joint angles. Additionally, rand is a random function that generates values within the range of [0, 1].

3) Use the for function to bring the obtained Angle into the end position vector to obtain the end position parameters of the modular robot arm.

The workspace of a modular robotic arm is a critical metric for evaluating its performance. In MATLAB, we employ the Monte Carlo method for programming simulation, as shown in Fig. 7 [21,22]. The workspace of the robotic arm, as depicted in Fig. 7, is generally maintained within a range of 600 millimeters, with the length of the wrist part being 600 millimeters. By analyzing the workspace, we can demonstrate that the design of the robotic arm is rational and meets the required workspace specifications [23-25].

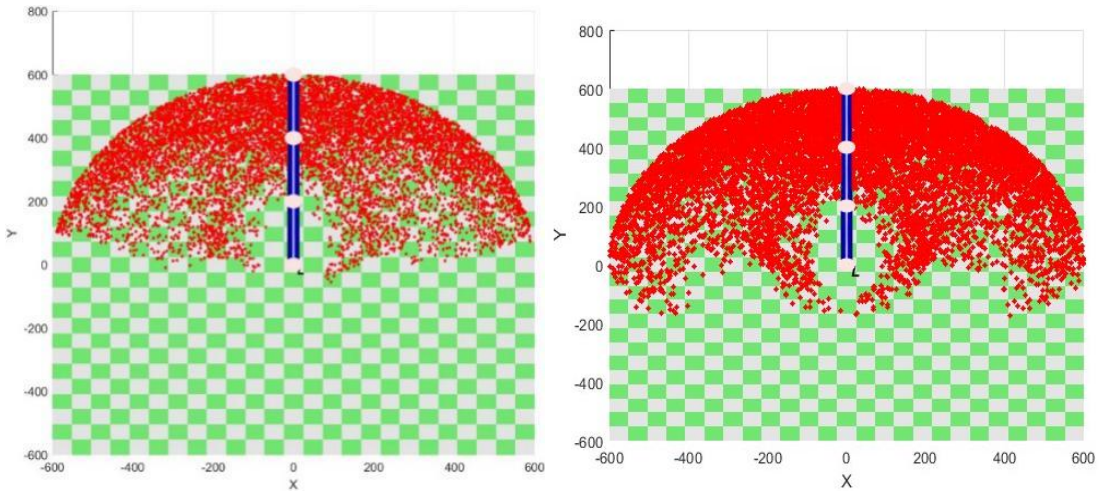

（A） （B）

Fig. 7. Robotic arm workspace set

Similarly, we employ the aforementioned method to simulate the motion space of a four-axis robotic arm. As shown in Fig. 7, due to the absence of constraints from an end posture retention mechanism, we can compare its workspace with that of the modular robotic arm. First, the end position is exported and calculated within MATLAB. Since the robotic arm is planar, we set the range of the end position values to [600,600,0], and ensure that the number of iterations is consistent when calculating the workspace for both types of robotic arms. Subsequently, the data points of both robotic arms within this range are exported to Excel. By utilizing the COUNTIF function in Excel, we calculate the number of points with a blank y-value and divide it by the total number of iterations. Using this method, we determine that the ratio of the motion space of the modular robotic arm to that of the four-axis robotic arm is 93%.

Export data for actual programming:

```
Clear

open('a1.fig');

handle = findobj(gca,'Type','line');
xdata = get(handle,'XData');
ydata = get(handle,'YData');
```

Calculate the ratio:

```
COUNTIF(B:B,"NAN")/COUNTA(B:B)
```

Thus, it can be observed that when a robotic arm is in a complex environment cluttered with obstacles, its movement may be restricted, and it might only be able to maintain a single state. In such cases, an end posture retention mechanism can be utilized to keep the end effector parallel to the working plane, allowing for operational tasks on the end effector.

5. EXPERIMENT

The measured total weight of the three-axis robot arm is 3.12kg. Because each robot arm has the same size and structure, the weight of a single robot arm is about 1kg. The mechanical arm is a series mechanical arm, so the center of gravity of the single segment of the mechanical arm can be approximated as the midpoint position, and the length of the single segment arm is 200mm. Each arm is treated as a separate connecting rod and the load torque of each section is calculated. Here are the calculation steps:

$$\tau = r \times F$$

Among them:

τ is the torque (unit: Newton meter, N·m),
r is the distance from the point of force to the axis of rotation (unit: m),
F is the force (Newton, N);

According to the control algorithm design described in part 2.3 of this paper, after the Arduino steering engine control and Matlab coordinate calculation and Angle conversion control programs are written, serial port communication is established for data transmission, and initial debugging is conducted in the upper electromechanical brain, the physical object is assembled for experimental debugging and motion display, and the overall motion diagram of the robot arm is shown. The result is shown in Figs. 8,9,10.

Similarly, because the structure and size of the robot arms at all levels are exactly the same, the decoupling accuracy of the robot arms at all levels tested in the experiment can be regarded as the module under different loads to decouple the robot arm, and the rotation results of the robot arms at all levels are summarized:

Table 3. List of class used for gravity to axis of rotation

Class	Weight per section (kg)	Gravity (N)	Distance from center of gravity to axis of rotation (m)	Load torque per section (N·m)
1	1	9.81	0.1	0.981
2	1	9.81	0.1	1.962
3	1	9.81	0.1	2.943

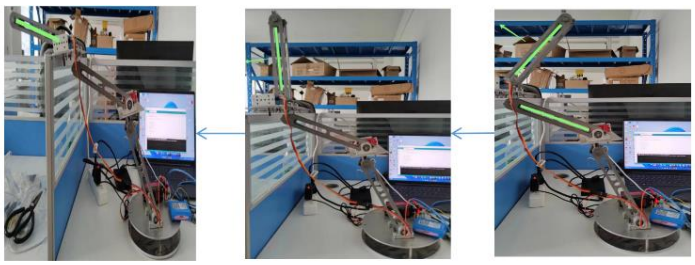

Fig. 8. First stage robotic arm rotation

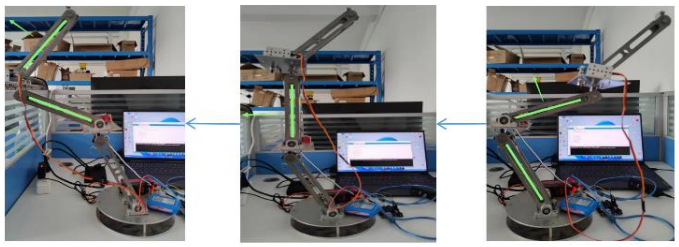

Fig. 9. Two stage robotic arm rotation

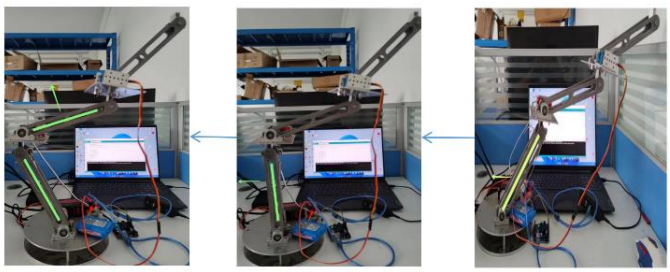

Fig. 10. Three stage robotic arm rotation

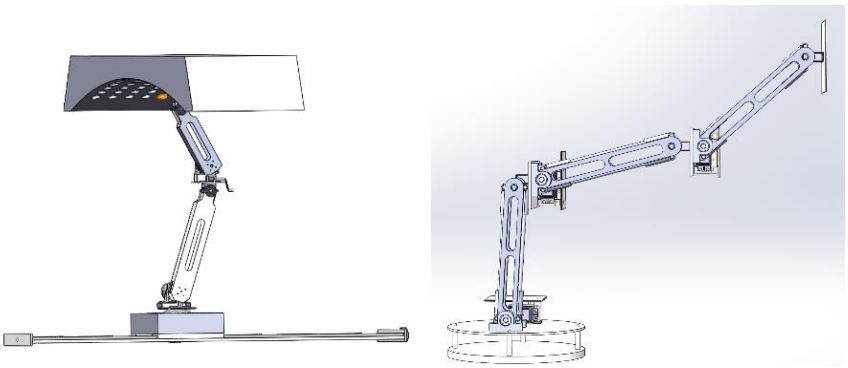

(a) **(b)**

Fig.11. Mechanical arm demonstrates

Table 4. Rotation results of the robot arms

Motion condition	The order of the robot arm	Primary Angle α_1	Primary Angle α_2	Present Angle α_1	Present Angle α_2	Attitude retention rate	Attitude retention rate
First stage	1	91	88	91.3	88	99.67%	100.00%
robotic arm	2	88	89	88	89	100.00%	100.00%
rotation	3	89	89	89	89	100.00%	100.00%
Two stage	1	87.8	88	88	88	99.77%	100.00%
robotic arm	2	88	89	88.4	90	99.55%	98.89%
rotation	3	89	89	90	90	98.89%	98.89%
Three	1	88	88	90	90	97.78%	97.78%
stage	2	88.3	88.6	89	89.3	99.21%	99.22%
robotic arm	3	89	89	90	90	98.89%	98.89%
rotation							

Table 5. The probability of maintaining the Angle of the working platform

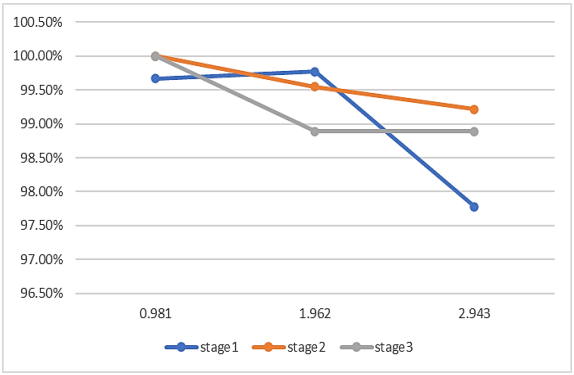

(α_1)

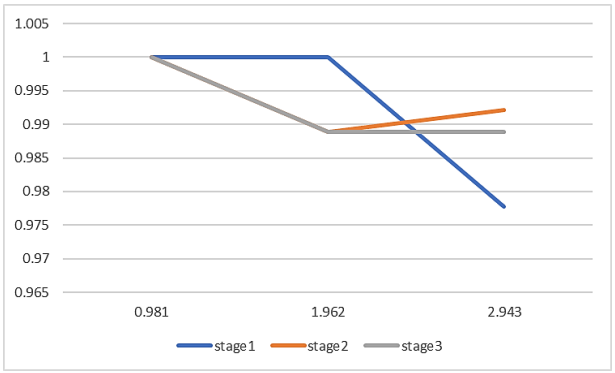

(α_2)

The Angle between the platform where the robot arm is located and the vertical ground direction is regarded as the measurement Angle α , the Angle between the low-end platform of the robot arm and the vertical ground direction is regarded as α_1 , the Angle between the top platform and the vertical ground direction is regarded as the measurement Angle α_2 , "Main Angle" indicates the target Angle set by the robotic arm before movement. "Current Angle" indicates the actual Angle reached by the robotic arm. "Attitude retention rate" shows how close the actual attitude of the robot arm is to the target attitude, calculated by the formula: (current Angle/main Angle) × 100%.

As can be seen from the table, with the increase of the order of the robot arm, the load of the robot arm also increases, and the attitude retention rate decreases slightly, but it remains above 97.78% in all tests, indicating that the robot arm can maintain good attitude control performance at all stages. The effectiveness of modular mechanical decoupling scheme is proved.

6. CONCLUSION

This paper specifically addresses the challenge of maintaining a stable end posture in multi-joint manipulators by conducting a comprehensive study on the design and simulation analysis of a modular parallel four-bar linkage robotic arm. A novel modularly decoupled mechanical arm has been researched, which simplifies the complexity of traditional manipulators while enhancing control precision and ensuring safety and automatic operation.

The study begins with an in-depth analysis of the motion mechanisms of the manipulator, deriving

the relationships between shape space, end position space, and the kinematics of forward and inverse movements. Utilizing the Robotic Toolbook in Matlab, a simulation model of the linkage manipulator was established, achieving structural simulation analysis and verifying the effectiveness of the kinematic equations. Through Matlab programming, the terminal positioning and posture control of different structural manipulators were simulated and compared. The results indicate that the modularly decoupled mechanical arm has the following advantages in the special workspace described in the paper: the modular design of the mechanical arm not only simplifies the mechanical structure but also expands the working range to a certain extent, providing a cost-effective solution by reducing the number of required motors. This approach significantly reduces the difficulty of control programming due to the independence of each arm level. The workspace of the manipulator was calculated using the Monte Carlo method and compared with that of traditional planar manipulators. The results emphasize the effectiveness of the kinematic equations and the ratio of the end working space. According to the experimental results, although the attitude retention rate will decrease with the increase of the load of the robot arm, it remains above 97.78% in all tests, indicating that the robot arm can maintain good attitude control performance at all stages, verifying the feasibility of the modular decoupling scheme. Despite the high attitude retention rate, there are still some errors, which may be due to a variety of factors, including but not limited to sensor accuracy, control algorithm accuracy, material elastic deformation, and external environment interference.

Further optimization and application directions include optimizing the structure and control algorithms of the modular mechanical arm based on specific application scenarios. As shown in Fig. 9, (a) depicts the modularly decoupled mechanical arm applied in roof chiseling operations, where by adding guide rails and a rotating base, the mechanical arm is converted from planar to spatial operation, increasing the working range and robustness. (b) Represents an optimization scheme suitable for vertical scenarios, which reduces the impact of the dead points often present in parallelogram structures. The above schemes can be applied to scenarios requiring stable end postures, such as concrete bridge chiseling and kiwi picking Fig. 11.

The proposed mechanical arm demonstrates advantages in reducing the complexity of control system design and supporting subsequent research and development. In conclusion, the modular parallel four-bar linkage robotic arm presented in this paper offers a practical and efficient solution for applications requiring precise end posture control. This research provides a theoretical foundation for the further development of the field of modularly decoupled mechanical arms.

DISCLAIMER (ARTIFICIAL INTELLIGENCE)

Author(s) hereby declare that NO generative AI technologies such as Large Language Models (ChatGPT, COPILOT, etc) and text-to-image generators have been used during writing or editing of manuscripts.

COMPETING INTERESTS

Authors have declared that no competing interests exist.

REFERENCES

1. Gerlind Wisskirchen, Blandine Thibault Biacabe, Ulrich Bormann. Artificial intelligence and robotics and their impact on the workplace. IBA Global Employment Institute; April 2017.
2. Abd-Elbadee Saeed Mohamed Abd-Elmohsin. Design and fabricate handling arm. Sudan University of Science and Technology; October 2016.
3. Suvitha S, Lillygrace C, Nandhini M, Nithyashree S. Implementation of robotic hand imitating the real time motions. International Journal of Innovative Research in Science, Engineering and Technology. 2019;8(3).
4. Guanqi Liang, Di Wu, Yuxiao Tu, Tin Lun Lam. Decoding modular reconfigurable robots: A survey on mechanisms and design. 2023; arXiv 2310.09743 Available:https://arxiv.org/abs/2310.09743
5. Feng Xu, Bin Zi, Zhaoyi Yu, Jiahao Zhao, Huafeng Ding. Design and implementation of a 7-DOF cable-driven serial spray-painting robot with motion-decoupling mechanisms,Mechanism and Machine Theory. 2024;192:105549. ISSN 0094-114X, Available:https://doi.org/10.1016/j.mechmachtheory.2023.105549.

6. Kinematic optimal design of a 2-degree-of-freedom 3-parallelogram planar parallel manipulator
7. Guangyu Zhang, Li Ruipeng, Yang Qihua, Gao Sheng. Establishment and analysis of kinematics and mechanics models of upper limb rehabilitation robotic arm. DOI:10.16652/j.issn.1004?373x.2024.14.023
8. Runtong Sun, Jun Wu, Yanling Tian. Control of a painting robot containing parallelogram linkages based on its distinctive dynamic characteristics, Mechanism and Machine Theory. 2024; 200:105702.ISSN 0094-114X Available:https://doi.org/10.1016/j.mechmachtheory.2024.105702
9. Wu G, Bai S. Design and kinematic analysis of a 3-RRR spherical parallel manipulator reconfigured with four–bar linkages. Robotics and Computer-Integrated Manufacturing. 2019 Apr 1;56: 55-65.
10. Perreault S, Cardou P, Gosselin C. Approximate static balancing of a planar parallel cable-driven mechanism based on four-bar linkages and springs. Mechanism and Machine Theory. 2014 Sep 1;79:64-79.
11. Liu Y, Ben-Tzvi P. Design, analysis, and integration of a new two-degree-of-freedom articulated multi-link robotic tail mechanism. Journal of Mechanisms and Robotics. 2020 Apr 1;12(2): 021101.
12. Khan WA, Tang CP, Krovi VN. Modular and distributed forward dynamic simulation of constrained mechanical systems–A comparative study. Mechanism and Machine Theory. 2007 May 1;42(5):558-79.
13. Khan WA, Krovi V. Comparison of two alternate methods for distributed forward dynamic simulation of a four-bar linkage. InProc. Workshop on Fundamental Issues and Future Research Directions for Parallel Mechanisms and Manipulators, Quebec; 2002.
14. Yao W, Dai JS. Workspace and orientation analysis of a parallel structure for robotic fingers. Journal of Advanced Mechanical Design, Systems, and Manufacturing. 2011;5(1):54-69.
15. MO Yi. D-H model and simulation analysis based on 6-DOF industrial robot [J]. Machine tool Chinese Journal of Hydraulic Engineering. 2017;45(11):64-68.
16. Ma Yuhao. Six-degree-of-freedom robotic arm obstacle avoidance trajectory planning and control algorithm research (Liu Zi You Du Ji Xie Bi Bi Zhang Gui Ji Ji Kong Zhi Suan Fa Yan Jiu) [D]. University of Chinese Academy of Sciences; 2019.
17. Zuo Fuyong, Hu Xiaoping, Xie Ke, et al. SCARA robot trajectory planning and simulation based on MATLAB Robotics toolbox (Ji Yu MATLAB Robotics Gong Ju Xiang De SCARA Ji Qi Ren Gui Ji Gui Hua Yu Fang Zhen) [J]. Haapasalo, Xiang Tan: Journal of Hunan University of Science and Technology. 2012;2:43-46.
18. Zhou Aiguo, Zhou Fei, Nv Gang, et al. Kinematics and workspace analysis of an articulated arm CMMJ(Guan Jie Bi Shi Zuo Biao Ce Liang Ji De Yun Dong Xue Yu Gong Zuo Kong Jian Fen Xi)[J]. Journal of Mechanical Drives. 2019;10.
19. Huayang Li, Chenkun Qi, Feng Gao, Xianbao Chen, Yue Zhao, Zhijun Chen. Mechanism design and workspace analysis of a hexapod robot. Mechanism and Machine Theory. 2022;174:104917. ISSN 0094-114X
20. Pawletta T, Freymann B, Deatcu C, Schmidt A. Robotic control & visualization toolbox for Matlab, IFAC-Papers OnLine. 2015;48(1):687-688. ISSN 2405-8963
21. Shi Y, Liu Y, Guo P. Kinematic analysis and control of the handling robotic arm. 7th international conference on advanced algorithms and control engineering (ICAACE), Shanghai, China. 2024;1402-1406. DOI:10.1109/ICAACE61206.2024.10549503.
22. Adrián Peidró, Óscar Reinoso, Arturo Gil, José María Marín, Luis Payá. An improved Monte Carlo method based on Gaussian growth to calculate the workspace of robots. Engineering Applications of Artificial Intelligence. 2017; 64:197-207. ISSN 0952-1976.
23. Eckenstein N, Yim M. Modular advantage and kinematic decoupling in gravity compensated robotic systems. Journal of Mechanisms and Robotics. 2013 Nov 1;5(4):041013.

24. Jing ZH, Dongbao WA, Guangping WU, Hongwei GU, Rongqiang LI. Mechanism design and motion analysis of heavy‐load transfer robot with parallel four‐Bar Mechanism. Transactions of Nanjing University of Aeronautics & Astronautics. 2022 Oct 1;39(5).

25. Jin S, Kim J, Bae J, Seo T, Kim J. Design, modeling and optimization of an underwater manipulator with four-bar mechanism and compliant linkage. Journal of Mechanical Science and Technology. 2016 Sep;30: 4337-43.

Peer-review history:
The peer review history for this paper can be accessed here:
https://www.sdiarticle5.com/review-history/121200